

Structural design of high-performance capacitive accelerometers using parametric optimization with uncertainties

André da Costa Teves, Cícero Ribeiro de Lima, Angelo Passaro & Emílio Carlos Nelli Silva

To cite this article: André da Costa Teves, Cícero Ribeiro de Lima, Angelo Passaro & Emílio Carlos Nelli Silva (2017) Structural design of high-performance capacitive accelerometers using parametric optimization with uncertainties, *Engineering Optimization*, 49:3, 365-380, DOI: [10.1080/0305215X.2016.1187975](https://doi.org/10.1080/0305215X.2016.1187975)

To link to this article: <https://doi.org/10.1080/0305215X.2016.1187975>



Published online: 03 Jun 2016.



Submit your article to this journal [↗](#)



Article views: 323



View related articles [↗](#)



View Crossmark data [↗](#)



Citing articles: 3 View citing articles [↗](#)

Structural design of high-performance capacitive accelerometers using parametric optimization with uncertainties

André da Costa Teves^a, Cícero Ribeiro de Lima^b, Angelo Passaro^c and Emílio Carlos Nelli Silva^a

^aDepartment of Mechatronics and Mechanical Systems Engineering, Escola Politécnica da Universidade de São Paulo, São Paulo, SP, Brazil; ^bSchool of Engineering, Modeling and Applied Sciences, UFABC, Santo André, SP, Brazil; ^cInstitute for Advanced Studies, DCTA, São José dos Campos, SP, Brazil

ABSTRACT

Electrostatic or capacitive accelerometers are among the highest volume microelectromechanical systems (MEMS) products nowadays. The design of such devices is a complex task, since they depend on many performance requirements, which are often conflicting. Therefore, optimization techniques are often used in the design stage of these MEMS devices. Because of problems with reliability, the technology of MEMS is not yet well established. Thus, in this work, size optimization is combined with the reliability-based design optimization (RBDO) method to improve the performance of accelerometers. To account for uncertainties in the dimensions and material properties of these devices, the first order reliability method is applied to calculate the probabilities involved in the RBDO formulation. Practical examples of bulk-type capacitive accelerometer designs are presented and discussed to evaluate the potential of the implemented RBDO solver.

ARTICLE HISTORY

Received 11 February 2015
Accepted 28 April 2016

KEYWORDS

Bulk-type capacitive accelerometers; MEMS; optimization; robust design; reliability

1. Introduction

An accelerometer is a kind of microelectromechanical system (MEMS) device capable of measuring acceleration. MEMS accelerometers for high-performance applications were reviewed by Krishnan *et al.* (2007), who conducted a comparative study of the characteristics of several commercial devices.

This work focuses on the design of capacitive accelerometers. The main advantages of such transduction mechanisms are that they have high sensitivity, good direct current (DC) response and noise performance, low temperature sensitivity and low power consumption.

The two most commonly adopted designs for capacitive accelerometers are those with sensitivity to accelerations parallel (Coulter *et al.* 2008) and perpendicular (Alvarez *et al.* 2009) to the silicon surface of the device. They are usually implemented by surface and bulk micromachining technology (Madou 2002), respectively. In bulk micromachined devices, owing to the presence of a large proof mass, higher resolution and greater sensitivity are achieved. Yazdi and Najafi (2000) proposed a combined approach to further improve the sensor performance. In this work, bulk micromachined devices are considered (see Figure 2).

The main feature that distinguishes one bulk-type design from another is the configuration of the beams that support the movable electrode. The flexibility of the beams allows the proof mass to move proportionally to the external acceleration and its displacement is estimated by the change in capacitance of the set. The proof mass can be supported by one or more straight cantilever beams

(Roylance and Angell 1979), by a torsion beam (Selvakumar, Ayazi, and Najafi 1996) or by folded beams (Qiao *et al.* 2009). Currently, full-bridge and highly symmetrical designs using four or more beams (Seidel *et al.* 1990) are the most popular since they lead to very low cross-axis acceleration sensitivity, which is undesirable for unidirectional sensors.

The operation of MEMS sensors depends on many performance requirements (sensitivity, bandwidth, footprint area, and so on), which are often conflicting. In the case of accelerometers, to achieve high sensitivity it is necessary to reduce the air gap between the sensory electrodes and increase the active area. However, reducing the air gap reduces the dynamic range of the sensor and increases the squeeze film damping (Bao and Yang 2007) and, consequently, reduces the response time of the sensor. Moreover, a very small gap, combined with a large moving mass and low spring constants, can reduce the pull-in voltage considerably (Kaajakari 2009), resulting in the collapse of the electrodes at low applied voltages.

In addition, owing to the complex manufacturing processes of MEMS sensors, each iteration in the prototype development is very expensive and, thus, trial-and-error methods are often prohibitive. For these reasons, optimization techniques are often applied to the design stage of MEMS sensors, aiming to reduce development time and costs, and simultaneously helping the designer to explore design trade-offs efficiently.

Most of the research on the optimization of capacitive microaccelerometers so far has been primarily focused on parametric analysis. Liu, Jiang, and Wang (2009) performed a robust optimization considering both bandwidth and sensitivity of a similar device, and Desrochers, Pasini, and Angeles (2010) first optimized the shape of the hinges used in their bulk design and then performed a multi-objective size optimization aiming to maximize the sensitivity and minimize the ratio between the first and the second natural frequencies to reduce off-axis sensitivity.

Mukherjee, Zhou, and Fedder (1999), Coultate *et al.* (2008) and Engesser *et al.* (2010) presented analytical models for a surface-micromachined accelerometer, by proposing optimized designs considering different requirements. Mukherjee, Zhou, and Fedder (1999) considered the minimization of the footprint area and noise and maximization of the sensitivity. Coultate *et al.* (2008) presented a robust design by considering the maximization of the full-scale range and minimization of the threshold acceleration. Finally, Engesser *et al.* (2010) aimed at minimizing the footprint area of the device, and proposed several techniques to more easily find the global minimum of optimization problems involving MEMS sensors.

Although the potential of MEMS to enable the development of new applications is widely recognized, this technology is not yet well established owing to reliability problems; that is, the devices can fail before the end of the required lifetime or their performance can degrade rapidly, falling below acceptable levels.

Uncertainties associated with the dimensions and the material properties of the microdevices (MEMS) are inevitable owing to several factors such as manufacturing imperfections, residual thermal stress, irregular surfaces and chemical contamination (Kovacs 1998). These uncertainties may produce tolerances higher than 10% (Madou 2002) of nominal values and, thus, they represent significant challenges for realistic prediction of the performance of microdevices. It is not always possible to restrict the manufacturing tolerances for more precise dimensions. In addition, the load to which the device is subjected may vary depending on environmental and operating conditions.

The difference between the expected and real performance of a device is even greater when it is optimized, because any excess of structural material should be removed, making the optimized device more susceptible to great uncertainty. Conventional design methodologies deal with the uncertainties through the use of safety factors. However, safety factors are calibrated for average design conditions and, therefore, cannot guarantee suitable reliability levels for specific design conditions.

Currently, two main methods of optimization are proposed to overcome this problem, considering the uncertainty effects more consistently: robust design optimization (RDO), which aims to minimize the dispersion of structural responses, measured by low-order statistical moments; and reliability-based design optimization (RBDO), which aims to maximize the performance with probabilistic

constraints, enabling the design of structures with specified failure probabilities. In other words, the concept of reliability (or the probability of failure) of the RBDO refers to the occurrence of extreme events, while the RDO refers to the low dispersion of structural responses even with a wide variation in the input parameters. A more detailed review of these two approaches is presented in Schuëller and Jensen (2008).

Two approaches can be adopted to formulate an RBDO problem. One is based on system reliability-based design optimization (SRBDO), in which a single constraint includes all failure events (Nguyen, Song, and Paulino 2010; Silva *et al.* 2010; Chun, Song, and Paulino 2015). The other is based on component reliability-based design optimization (CRBDO), in which each probabilistic constraint is related to a unique failure event (Maute and Frangopol 2003; Allen *et al.* 2004; Kharmanda *et al.* 2004). Here, the latter is adopted, since it can be implemented with less computational cost.

In this work, the RBDO is applied to optimize the structure of a MEMS capacitive accelerometer. A parametric optimization algorithm has been developed, in which the uncertainties involved in the optimization problem, such as variations in geometric and material properties, are considered. To the authors' knowledge, the MEMS capacitive accelerometer structural design (as presented here) using RBDO has not been presented in any previous work in the literature. Therefore, the application of the RBDO algorithm is highlighted because it allows additional control over the reliability of the microsystem (MEMS capacitive accelerometer), by considering uncertainties in the geometric and material properties of the accelerometer design.

This article is organized as follows. In Section 2, a typical RBDO problem and the methodologies employed to evaluate efficiently the probabilistic constraints are briefly presented. In Section 3, the numerical implementation is addressed. In Section 4, the results are presented. Finally, Section 5 provides the concluding remarks and points to future developments. The Appendix shows the sensitivity analysis required for an RBDO problem.

2. Reliability-based design optimization: typical formulation

The optimization problem with uncertainties may include deterministic and probabilistic design criteria, which are mostly incorporated in the constraints of the problem. Probabilistic design criteria restrain a specific probability of failure, and it may also be present in the objective function. A typical RBDO formulation is given by:

$$\begin{aligned}
 &\underset{\mathbf{r}, \mathbf{s}}{\text{Minimize}} && \text{Prob}(c(\mathbf{s}, \mathbf{r}) \geq \bar{c}) \\
 &\text{Subject to} && \bar{P}_i - \text{Prob}(f_i(\mathbf{s}, \mathbf{r}) < 0) \geq 0, \quad i = 1, \dots, n \\
 &&& g_j(\mathbf{s}) \geq 0, \quad j = 1, \dots, m \\
 &&& \mathbf{s}_{\text{low}} \leq \mathbf{s} \leq \mathbf{s}_{\text{upp}}
 \end{aligned} \tag{1}$$

where \mathbf{r} are the random variables, n is the number of probabilistic constraints, and m is the number of deterministic constraints. The goal is to minimize the probability of the cost function $c(\mathbf{s}, \mathbf{r})$ to be greater than \bar{c} . One set of constraints $(1, \dots, n)$ restrains the probability of failure associated with the limit state functions $f_i(\mathbf{s}, \mathbf{r})$, where $f_i < 0$ means a failure situation. \bar{P}_i is the maximum acceptable probability of failure. Another set of constraints, g_j ($j = 1, \dots, m$), contains all deterministic constraints. In this generic formulation, the design variables \mathbf{s} can be deterministic or non-deterministic; that is, these variables should be a characteristic parameter of a statistical distribution, such as the mean or the standard deviation.

In the solution of problem (1), a major difficulty is finding the probability density function (PDF), associated with $c - \bar{c}$ (objective function) or f_i (constraints of the problem), explicitly in the random variables \mathbf{r} . In this case, two approximation methods are often applied: stochastic simulations, such as Monte Carlo (Kroese, Taimre, and Botev 2011), or the method of moments (Hasofer and Lind 1974). The calculation of the probability by simulations is very time consuming, so it is not useful for

optimization algorithms (Aoues and Chateauneuf 2010). Thus, in this work, the first order reliability method (FORM) and the concept of reliability index β are applied for the calculation of probabilities.

In addition, Liu and Kiureghian (1991) proved the robustness and efficiency of the Hasofer–Lind–Rackwitz–Fiessler (HL-RF) algorithm (Hasofer and Lind 1974) for solving a nonlinear optimization problem in the most probable failure point (MPFP; the region that gives the largest contribution to the probability of failure) with an equality constraint. This algorithm has been adopted in the present work. The formula for updating this algorithm is given by:

$$\mathbf{u}^{(k+1)} = \frac{G_{\mathbf{u}^{(k)}}^T \mathbf{u}^{(k)} - Q(\mathbf{u}^{(k)})}{G_{\mathbf{u}^{(k)}}^T G_{\mathbf{u}^{(k)}}} G_{\mathbf{u}^{(k)}} \quad (2)$$

where $G_{\mathbf{u}^{(k)}} = \{\partial Q/\partial u_1, \partial Q/\partial u_2, \dots, \partial Q/\partial u_n\}$ is the gradient of the limit state function Q with respect to \mathbf{u} at iteration k .

Several iterations using Equation (2) are required to find the failure surface, and consequently to determine the location of the MPFP along this failure surface.

An overview of the FORM procedure is illustrated in Allen *et al.* (2004), which sums up what has been discussed so far, as follows. First, the random variables (\mathbf{r}) must be mapped to the normalized space (\mathbf{u}) through a transformation, which makes the middle point in r -space correspond to the origin in u -space. For general cases, the principle of a normal tail (Madsen and Krenk 2006) can be applied to perform this transformation. Thus, the probability of failure is found by integrating the first order approximation of the limit state function on the MPFP.

Now, by adopting the same procedure for calculation of probabilities of the optimization problem given by Equation (1), one MPFP and one reliability index β are obtained for each probability constraint, as well as for the objective function. In the RBDO theory, this approach is known as the reliability index approach (RIA) (Enevoldsen and Sørensen 1994). In this approach, the optimization problem (1) is usually rewritten as follows:

$$\begin{aligned} &\text{Minimize}_{\mathbf{r}, \mathbf{s}} \quad \beta(c(\mathbf{s}, \mathbf{r}) \geq \bar{c}) \\ &\text{Subject to} \quad \beta(f_i(\mathbf{s}, \mathbf{r}) > 0) - \bar{\beta}_i \geq 0, \quad i = 1, \dots, n \\ &\quad \quad \quad g_i(\mathbf{s}) \geq 0, \quad j = 1, \dots, m \\ &\quad \quad \quad \mathbf{s}_{\text{low}} \leq \mathbf{s} \leq \mathbf{s}_{\text{upp}} \end{aligned} \quad (3)$$

where $\bar{\beta}_i$ is the minimum reliability index required.

For cases in which the failure surface is far from the origin of the normalized space, the RIA is often affected by convergence problems (Maute and Frangopol 2003). Thus, the performance measure approach (PMA) has also been proposed for RBDO in the literature (Tu, Choi, and Park 1999). The PMA is based on the following principle: minimizing a complex function under simple constraints is more efficient than minimizing a simple function under complex constraints (Aoues and Chateauneuf 2010). Thus, in this approach an optimization problem is solved in the normalized space, for a given required reliability index $\bar{\beta}$.

The value of the limit state function at the optimum solution of this optimization problem represents the worst performance for the required reliability index $\bar{\beta}$. This result is known as the minimum performance target point (MPTP). The robustness of the PMA is established, and it is consistent with the conventional RIA (Lee, Yang, and Ruy 2002). An inverse reliability analysis is carried out for calculating the MPTP.

As the reliability requirements have been assured in the inverse reliability analysis, the optimization problem with the PMA is usually set as follows:

$$\begin{aligned}
 &\underset{\mathbf{r}, \mathbf{s}}{\text{Minimize}} && f_c(\mathbf{s}, \mathbf{r}) \\
 &\text{Subject to} && f_i(\mathbf{s}, \mathbf{r}) \geq 0, \quad i = 1, \dots, n \\
 &&& g_j(\mathbf{s}) \geq 0, \quad j = 1, \dots, m \\
 &&& \mathbf{s}_{\text{low}} \leq \mathbf{s} \leq \mathbf{s}_{\text{upp}}
 \end{aligned} \tag{4}$$

where the performances of the objective function (f_c) and of the probabilistic constraints are measured with respect to distinct required reliability indices. Since a poor performance indicates the occurrence of failure, its signal at the MPTP can be used to determine whether the probability constraint is satisfied or not.

3. Numerical implementation

The algorithm of the reliability-based optimization solver, implemented in this work using MATLAB® code, is illustrated in Figure 1.

First, all known structural geometric data of the accelerometer should be provided to the RBDO solver. These input data are used as the initial value of the design variables. After that, all information about the statistical distributions governing the uncertainties of the problem should also be provided, such as the type of distribution and statistical parameters (mean and standard deviation for the normal distribution, for instance).

As depicted in the flowchart of Figure 1, the algorithm of the implemented solver is structured in two nested loops. The reliability analyses are carried out in the inner loop, and are employed as input data to the optimization process of the outer loop. In the inner loop, which occurs in normalized space, structural analyses are done to carry out several iterations of Equation (2) until the probabilistic constraint values can be estimated in terms of the reliability index for the RIA or the performance target for the PMA.

The parametric optimization algorithm based on RBDO, implemented in this work, requires the calculation of the derivatives (or gradients) of the objective function and constraints, which are known as sensitivity analyses. Since the FORM approach has been adopted, the sensitivity of probabilistic criteria can be calculated analytically (Allen and Maute 2004).

The objective function and any deterministic constraints, as well as their sensitivity analyses, are provided to the optimizer of the outer loop. In this work, the method of moving asymptotes (MMA) (Svanberg 1987) is used as the optimizer for updating the values of the design variables. The implemented solver of this work is validated by comparison with the work of Lee, Yang, and Ruy (2002).

4. Results

The geometry shown in Figure 2 is used as a reference (initial guess) in the optimization problem presented in this section. This suggested geometry (Figure 2), the dimensions of which are presented in Table 1, has been employed as a spring for a high-performance accelerometer (Rodrigues *et al.* 2011).

The design of the accelerometer has three thick silicon wafers, bonded one on top of another. The intermediate layer consists of a proof mass suspended by flexible beams. It is separated from the top and bottom wafers by a small gap, resulting in two sets of parallel plate capacitors. The three silicon wafers have orientation (100) and a thin layer of silicon oxide (Figure 2b) is used as the electrical insulation between them. Some specifications have been employed for the accelerometer, focusing on unmanned aerial vehicles, such as sensitivity (500 mV/g), operating temperature (45–125°C), width

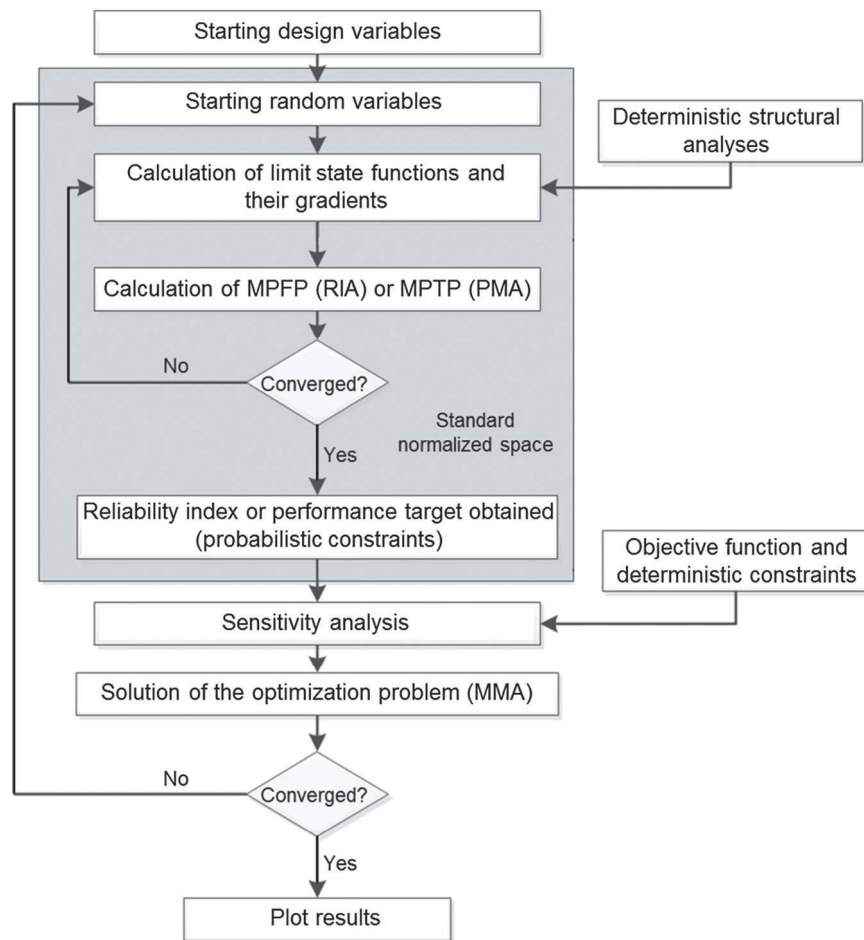


Figure 1. Flowchart of the optimization algorithm. MPFP = most probable failure point; RIA = reliability index approach; MPTP = minimum performance target point; PMA = performance measure approach; MMA = method of moving asymptotes.

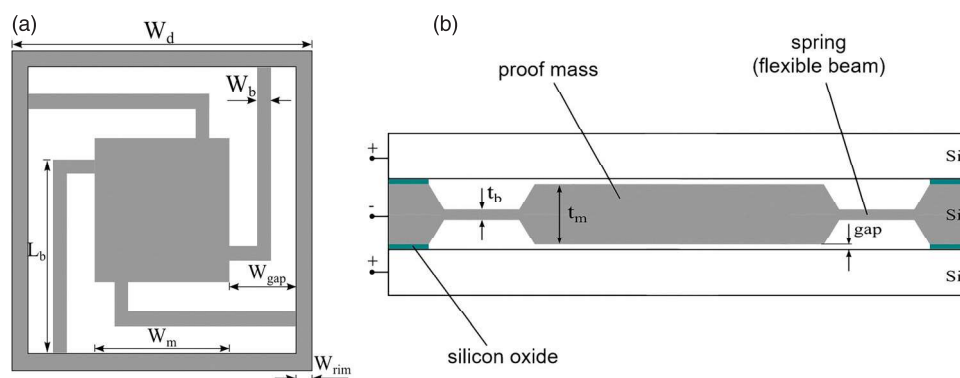


Figure 2. Original spring structure designed for a high-performance accelerometer: (a) top view; (b) cross-section view.

Table 1. Dimensions of the suggested geometry (Figure 1) adopted as reference.

Parameter	Description	Value (μm)
W_m	Proof mass width	2000
t_m	Proof mass thickness	380
W_b	Flexible beam width	200
t_b	Flexible beam thickness	55
L_b	Flexible beam length	2820
gap	Void space	2
W_{gap}	Distance between proof mass and outline	1040
W_{rim}	Outline width	150
W_d	Width of the device	4380

band (400 Hz) and footprint area that allows it be encapsulated in a 20-pin low-temperature cofired ceramic (LTCC) (Rodrigues *et al.* 2011).

In this work, only the geometry of the mechanical system is optimized, without considering any aspects of the electronic or control systems of the accelerometer. The effects of temperature change, such as thermal expansion, are also not considered here. Initially, a study of deterministic parametric optimization is carried out; that is, without any random variable in the problem. Then, different uncertainties and reliability levels are specified and the results of the RBDO are compared with the initial design and the deterministic optimum solution. The structural analyses required for these studies are based on analytical formulae found in Rodrigues *et al.* (2011), which evaluate the resonance frequency (f_n) and sensitivity (S_e) of high-performance accelerometers.

4.1. Deterministic solution

As mentioned previously, having a small footprint area is an important requirement for the accelerometer, to allow it be encapsulated in a 20-pin LTCC (Rodrigues *et al.* 2011). Therefore, to achieve a large reduction in the width of accelerometer device, the deterministic optimization problem is stated as:

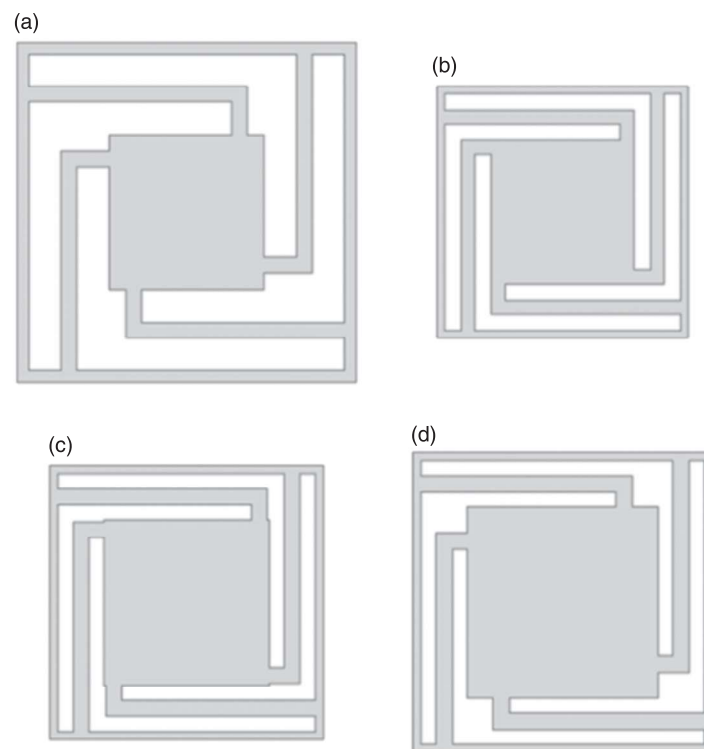
$$\begin{aligned}
 &\text{Minimize} && W_d = W_m + 2W_{\text{gap}} + 2W_{\text{rim}} \\
 &\text{Subject to} && f_n \geq 2500\text{Hz} \\
 &&& S_e \geq 0.6\text{pF/g} \\
 &&& \mathbf{s}_{\text{low}} \leq \mathbf{s} \leq \mathbf{s}_{\text{upp}}
 \end{aligned} \tag{5}$$

where the width (W_d) of the suggested structure (Figure 2) is adopted as the objective function. In addition, lower limits for the first resonance frequency ($f_n = 2500\text{ Hz}$) and for the sensitivity ($S_e = 0.6\text{ pF/g}$) of the accelerometer have been considered as constraints. The dimensions shown in Table 1 have been adopted as initial values for the optimization process. Table 2 shows all the design variables (\mathbf{s}) adopted in the deterministic optimization, as well as the lower (\mathbf{s}_{low}) and upper (\mathbf{s}_{upp}) limits, and the optimized values obtained by the deterministic problem (5). A comparison of the original design (Figure 2) proposed for the accelerometer (Rodrigues *et al.* 2011) and the optimized geometric configuration obtained by the deterministic problem can be seen in Figure 3.

Thus, a decrease of approximately 26% in the width of the device is concluded by the deterministic optimization problem. Despite this significant reduction in the width of the device, it is observed that a reliability of 56.10% has been found for the original design of the accelerometer (Rodrigues *et al.* 2011), while the reliability of the optimized result by deterministic problem can be considered to be only 50%. This result reinforces the warning made previously about the deterministic optimization; that is, when a structure is optimized, any excess of material is generally removed, making it even more susceptible to the uncertainties present in the manufacturing processes or the final application.

Table 2. Upper and lower limits of the dimensions adopted as design variables.

Design variable (s)	Lower limit (s_{low}) (μm)	Upper limit (s_{upp}) (μm)	Optimized solution (s^*)
W_m	500	2500	1847
t_m	250	500	405
W_b	100	300	179
t_b	10	100	46
L_b	2000	3000	2447
Gap	2	10	2
W_{gap}	600	1200	600
W_{rim}	100	200	100

**Figure 3.** Optimized geometric configurations and comparison among results: (a) original design (Figure 2); (b) result obtained with a deterministic problem; (c) result obtained with a reliability-based design optimization (RBDO) problem for $\bar{\beta} = 1$; (d) result obtained with an RBDO problem for $\bar{\beta} = 2$.**Table 3.** Statistical distribution associated with the silicon properties of the accelerometer (original design adopted as reference).

Statistical parameter	Statistical distribution	Mean (μ)	CoV
E : Young's modulus (GPa)	Normal	170	0.10
ρ : Density (kg/m^3)	Normal	2330	0.10

Note: CoV = coefficient of variation.

4.2. Reliability-based design optimization with material uncertainties

Now, the RBDO problem is carried out, considering the material properties of the accelerometer as uncertainties (\mathbf{r}). The uncertainties are considered as Gaussian variables with the adopted statistical parameters presented in Table 3. All other parameters are kept identical to the previous optimization problem (deterministic case).

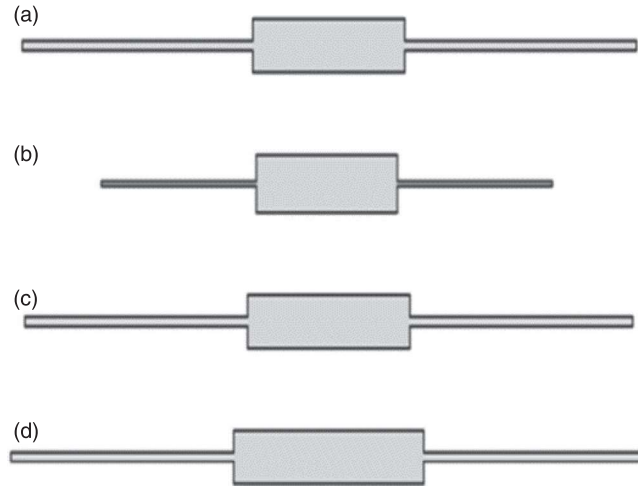


Figure 4. Optimized cross-section configurations and comparison among results: (a) original design of the accelerometer ($\bar{\beta} = 0.15$); (b) result obtained with a deterministic problem ($\bar{\beta} = 0$); (c) result obtained with a reliability-based design optimization (RBDO) problem for $\bar{\beta} = 1$; (d) result obtained with an RBDO problem for $\bar{\beta} = 2$.

Thus, using the RIA, the new optimization problem is set as follows:

$$\begin{aligned}
 &\text{Minimize} && W_d \\
 &\text{Subject to} && \beta(f_n(\mathbf{s}, \mathbf{r}) \geq 2500) - \bar{\beta} \geq 0 \\
 &&& \beta(S_e(\mathbf{s}, \mathbf{r}) \geq 0.6) - \bar{\beta} \geq 0 \\
 &&& \mathbf{s}_{\text{low}} \leq \mathbf{s} \leq \mathbf{s}_{\text{upp}}
 \end{aligned} \tag{6}$$

where two different $\bar{\beta}$ (minimum reliability index required) are evaluated: $\bar{\beta} = 1$ and $\bar{\beta} = 2$, which represent reliabilities of 84.13% and 97.72%, respectively.

It is observed that convergence of the RBDO algorithm has failed for reliability levels higher than the value corresponding to $\bar{\beta} = 2$, owing to the limit values applied to the constraints. Statistical properties of the random variables, shown in Table 3, have been chosen arbitrarily. Thus, if these parameters could be more accurately estimated, higher reliability indices should be achieved. The results obtained for the two values of the reliability index are shown in Figures 3 and 4. For comparison, Table 4 summarizes the results obtained for the deterministic optimization and the RBDO approach, including the results of the original design proposed for the accelerometer.

The values of f_n and S_e presented in Table 4 are calculated using the average value of the Young's modulus and density of the silicon and, for this reason, they are larger than the specified minimum value when higher levels of reliability are employed. In other words, the probabilistic constraints are far from boundary of the feasible domain for higher levels of reliability.

In Table 4, the width value of the device (W_d) is explicitly given only for the original geometry (Figure 2), and for all other cases it is given as the percentage reduction from the original geometry. As expected, larger values of the reliability index ($\bar{\beta}$) produce a smaller reduction in the size of the device. However, this result is increasingly robust to the inherent variations in material properties.

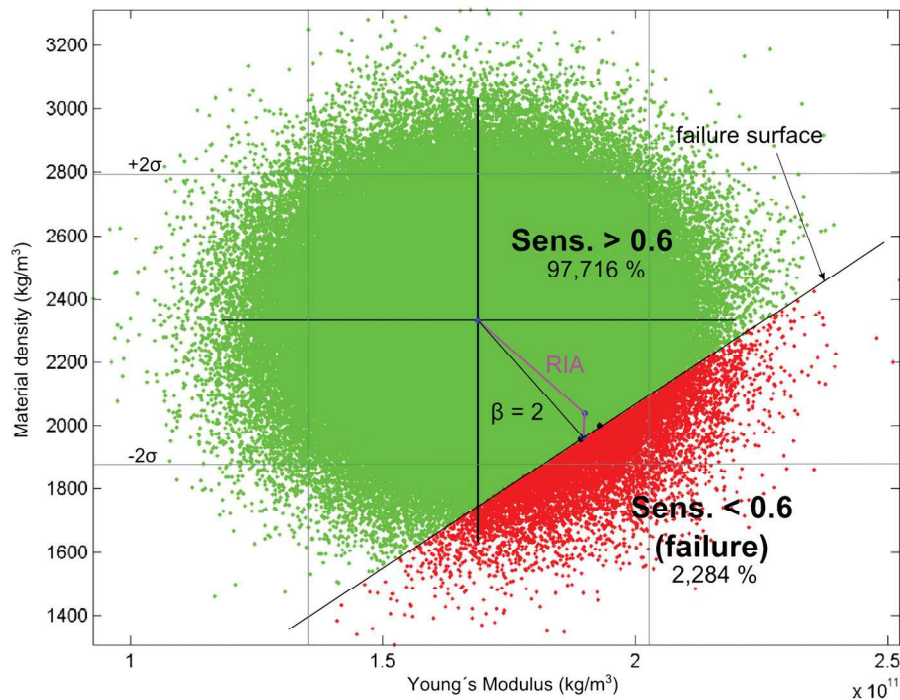
It is noticed that, with the constraints employed here, the geometry of the optimized result is approximately 12% lower than the original design, while the reliability has increased to 97.72%; that is, for every 100 manufactured devices, at most three cannot achieve the resonance frequency and sensitivity requirements.

To validate the results presented in Figures 3 and 4, the Monte Carlo method is applied to calculate the probability of failure of the optimized configuration obtained by the implemented RBDO

Table 4. Results of the parametric optimization with and without reliability.

	Original design	Deterministic solution	RBDO solution for $\bar{\beta} = 1$	RBDO solution for $\bar{\beta} = 2$
W_m	2000	1847	2129	2464
t_m	380	405	380	361
W_b	200	179	200	215
t_b	55	46	55	61
L_b	2820	2447	2706	2733
Gap	2	2	2	2
W_{gap}	1040	600	600	600
W_{rim}	150	100	100	100
f_n (Hz)	2678	2500	2684	2886
S_e (pF/g)	0.60	0.60	0.69	0.80
W_d	4380	-25.8%	-19.4%	-11.8%
Reliability	56.1%	50%	84.13%	97.72%

Note: RBDO = reliability-based design optimization.

**Figure 5.** Result obtained from probability calculation of the sensitivity constraint using the Monte Carlo method. RIA = reliability index approach.

algorithm, when $\bar{\beta} = 2$. Figures 5 and 6 and Table 5 summarize the results of this analysis, in which 225,000 samples were used and a total computational time of approximately 35 min was required, using a computer (Intel Core i7-16, with GB RAM) running the Windows operating system.

In Figures 5 and 6, the two perpendicular central lines represent the average value of the random variables E and ρ , and the lighter lines indicate two standard deviations (2σ) of the mean (μ). Figures 5 and 6 also illustrate the history of iterations by the RIA and the location of the MPFP.

By evaluating the obtained results, it can be stated that despite the FORM using the RIA being a rough and simple method for the calculation of probabilities, it is extremely effective for the problem considered here. The probability values obtained by this methodology are almost coincident with those obtained by the Monte Carlo method, but with much lower computational cost. As can be seen

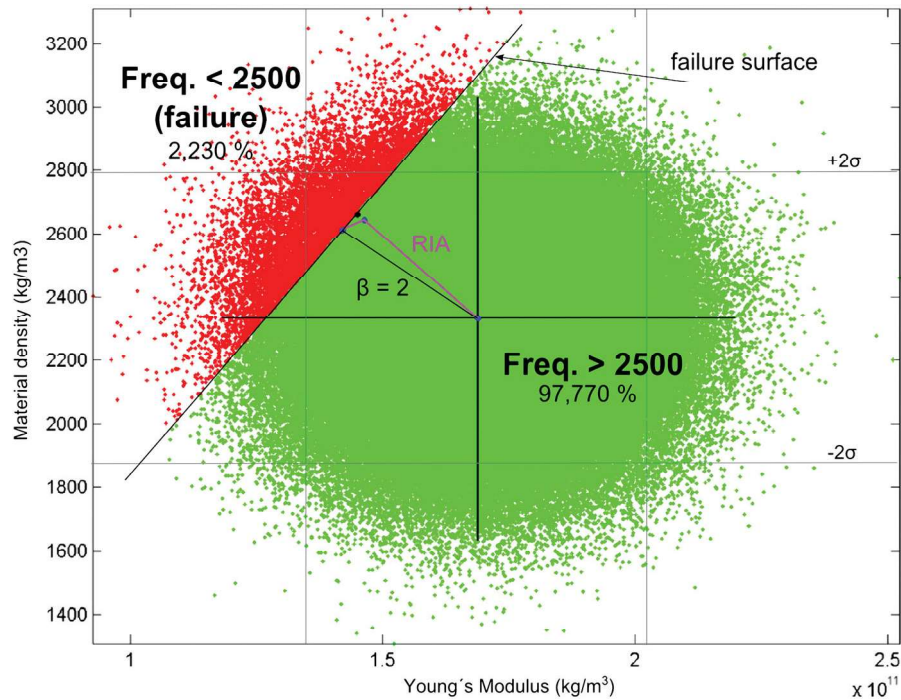


Figure 6. Result obtained from probability calculation of the resonance frequency constraint using the Monte Carlo method. RIA = reliability index approach.

Table 5. Comparison between reliability values obtained by the reliability index approach (RIA) and Monte Carlo method.

Constraint	RIA (%)	Monte Carlo method (%)
Sensitivity	97.72	97.72
Resonance frequency	97.72	97.70

in Figures 5 and 6, both limit state functions are practically linear, especially in the neighbourhood of the MPFP, which justifies the use of the FORM.

It is observed that despite the influence of the parameters E and ρ being not linear for the calculation of sensitivity and resonance frequency, this does not necessarily imply that the limit state function is nonlinear in the space of random variables.

4.3. Reliability-based design optimization with material and geometry uncertainties

Finally, a case study closer to a real-world scenario is presented here. In addition to uncertainties associated with the material properties, in this study one of the design variables is considered as a random variable.

The thickness of the flexible beam (t_b) connected to the proof mass (Figure 2) was chosen as a random design variable, because both the resonance frequency and sensitivity of the device are strongly influenced by this parameter, as verified experimentally. In this example, this variable is represented by the mean of the statistical distribution (μ_{t_b}). The other dimensions of the device showed very little variation between the design value and the value obtained experimentally and, therefore, they will be treated as deterministic variables in this example.

Table 6. Statistical distribution and design variables of the problem.

Statistical parameter	Statistical distribution	Mean (μ)	CoV
E : Young's modulus (GPa)	Normal	170	0.02
ρ : Density (kg/m ³)	Normal	2330	0.02
t_b : Beam thickness (μm)	Normal	μ_{tb} (design variable)	0.05

Note: CoV = coefficient of variation.

Table 7. Upper and lower limits of the adopted design variables.

Design variable	Lower limit (s_{low}) (μm)	Upper limit (s_{upp}) (μm)
W_m	500	3000
t_m	250	500
L_b	2000	3000
Gap	2	10
W_{gap}	600	1200
W_{rim}	100	200
$E(t_b)$	10	100

Table 8. Results of the parametric optimization with uncertainties in geometric and material properties.

	Original design	RBDO solution for $\bar{\beta} = 1$	RBDO solution for $\bar{\beta} = 2$
W_m	2000	2261	2771
t_m	380	364	343
W_b	200	182	204
t_b	55	61	68
L_b	2820	2748	2663
Gap	2	2	2
W_{gap}	1040	600	600
W_{rim}	150	100	100
f_n (Hz)	2678	2775	3092
S_e (pF/g)	0.60	0.73	0.88
W_d	4380	−16.4%	−4.8%
Reliability	56.1%	84.13%	97.72%

Note: RBDO = reliability-based design optimization.

For simplicity, and based on the fabrication process and some experimental results, $W_b = 3t_b$ is considered in this example. Although there are additional fabrication constraints for the device, only this one ($W_b = 3t_b$) will be considered here. Table 6 shows the statistical parameters adopted in this example, and Table 7 presents the design variables and their respective upper and lower limits. All other specifications are kept identical to the examples previously evaluated.

Table 8 presents the optimized results obtained for $\bar{\beta} = 1$ and $\bar{\beta} = 2$, which represent reliabilities of 84.13% and 97.72%, respectively. No convergence was found for reliability levels higher than 97.72% ($\bar{\beta} = 2$). Thus, the PMA was applied for the calculation of probabilities of the problem. Figures 7 and 8 compare the different optimized solutions obtained so far. In both figures, only results obtained by the RBDO problem with $\bar{\beta} = 2$ are used for this comparison. Thus, Figures 7(c) and 8(c) show again the results obtained by considering uncertainties in the material properties, presented in Section 4.2, while Figures 7(d) and 8(d) show the results obtained considering also uncertainties in thickness t_b .

For the highest level of reliability ($\bar{\beta} = 2$), it is noticed that size of the device (W_d) is approximately equal to the initial design, where a 4.8% reduction with respect to the original design can be seen. However, the dimensions of the geometry are considerably different, which indicates that the simple reallocation of mass in certain regions of the device seems to be sufficient to significantly increase its reliability.

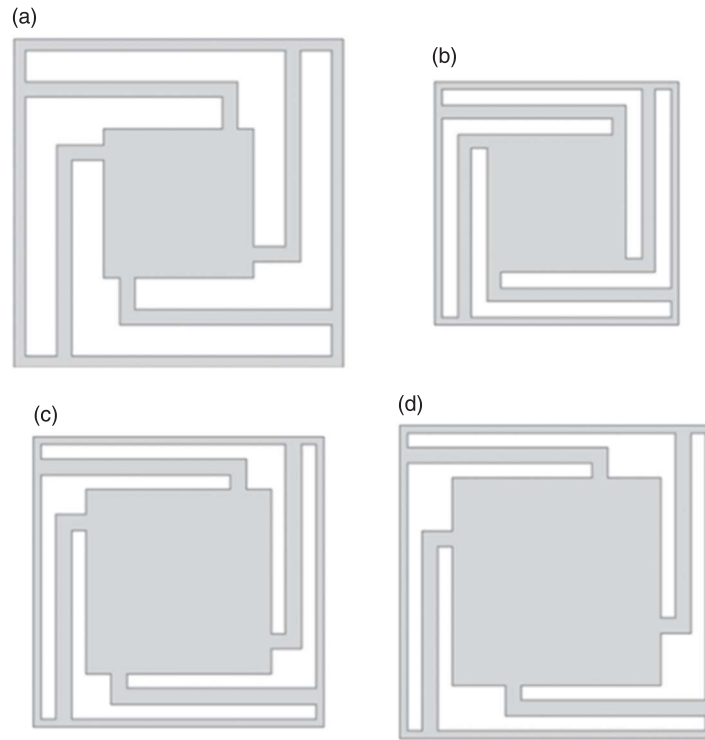


Figure 7. Comparison among optimized solutions: (a) original design (Figure 2); (b) result obtained with deterministic problem; (c) result obtained with RBDO problem for uncertainties in material properties (case 1; $\bar{\beta} = 2$); (d) result obtained with RBDO problem for uncertainties in geometric and material properties (case 2; $\bar{\beta} = 2$).

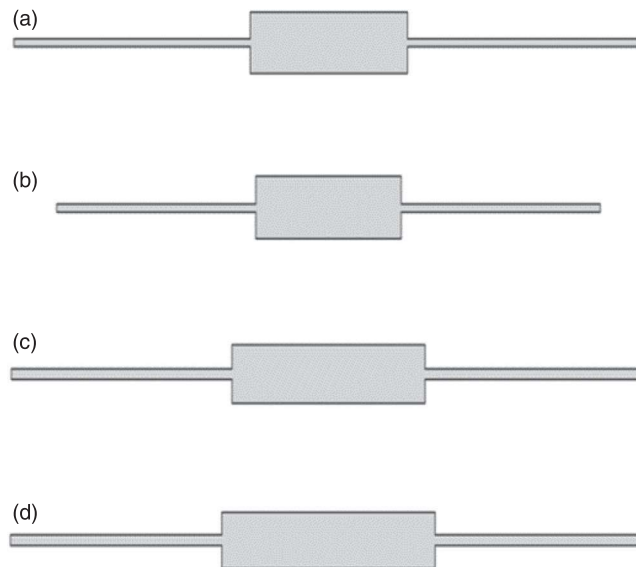


Figure 8. Comparison among optimized cross-section configurations: (a) original design of the accelerometer ($\bar{\beta} = 0.15$); (b) result obtained with a deterministic problem ($\bar{\beta} = 0$); (c) result obtained with a reliability-based design optimization (RBDO) problem with uncertainties in material properties (case 1; $\bar{\beta} = 2$); (d) result obtained with an RBDO problem for uncertainties in geometric and material properties (case 2; $\bar{\beta} = 2$).

5. Conclusions

A methodology for the design of MEMS capacitive accelerometers, based on a parametric RBDO approach, is presented and evaluated using some examples, including a case study with the original design of a high-performance capacitive accelerometer device.

Two different approaches, RIA and PMA, are applied to the FORM of the RBDO solver implemented in this work. Nevertheless, despite the FORM using RIA being a rough and simple method for the calculation of probabilities, it is extremely effective for the problems considered in this work. RIA has better convergence to search an optimized solution for RBDO problems, except for cases in which material and geometric uncertainties are considered simultaneously, and higher reliability levels (more than 97.72%) are required.

Finally, it is important to mention that the statistical properties of the random variables have been chosen arbitrarily. Thus, a natural and very important extension to this work is the fabrication of the devices designed here, aiming to validate experimentally these results. However, before the accelerometer is fabricated, all the random variables involved in the optimization problems should be properly estimated. Therefore, it is suggested that for future experimental work, a careful study of this effect on accelerometer design could benefit effectively from this work.

Moreover, the SRBDO approach (Nguyen, Song, and Paulino 2010; Chun, Song, and Paulino 2015), which takes into account the system probability of failures, may be tried as a good alternative to provide optimized structural designs for the accelerometer studied here and, thus, to improve the accuracy in satisfying the probabilistic constraints.

Disclosure statement

No potential conflict of interest was reported by the authors.

Funding

The first author acknowledges the scholarship support provided by the Brazilian Agency for Funding of Studies and Projects (FINEP) [grant no. 01.09.0395.00]. The authors thank the National Council for Research and Development (CNPq) for financial support [grant nos 559908/2010-5, 310578/2012-4, 305782/2012-6 and 304121/2013-4]. Moreover, the authors are grateful to Krister Svanberg from KTH Royal Institute of Technology for supplying the MMA code.

References

- Allen, M., and K. Maute. 2004. "Reliability-Based Design Optimization of Aeroelastic Structures." *Structural and Multidisciplinary Optimization* 27: 228–242.
- Allen, M., M. Rauli, K. Maute, and D. M. Frangopol. 2004. "Reliability-Based Analysis and Design Optimization of Electrostatically Actuated MEMS." *Computers & Structures* 82 (13-14): 1007–1020.
- Alvarez, M. J., N. Gil-Negrete, L. Ilzarbe, M. Tanco, E. Viles, and A. Asensio. 2009. "A Computer Experiment Application to the Design and Optimization of a Capacitive Accelerometer." *Applied Stochastic Models in Business and Industry* 25 (2): 151–162.
- Aoues, Y., and A. Chateauneuf. 2010. "Benchmark Study of Numerical Methods for Reliability-Based Design Optimization." *Structural and Multidisciplinary Optimization* 41: 277–294.
- Bao, M., and H. Yang. 2007. "Squeeze Film Air Damping in MEMS." *Sensors and Actuators A: Physical* 136 (1): 3–27.
- Chun, J., J. Song, and G. H. Paulino. 2015. "Parameter Sensitivity of System Reliability Using Sequential Compounding Method." *Structural Safety* 55: 26–36.
- Coultate, J. K., C. H. Fox, S. McWilliam, and A. R. Malvern. 2008. "Application of Optimal and Robust Design Methods to a MEMS Accelerometer." *Sensors and Actuators A: Physical* 142 (1): 88–96.
- Desrochers, S., D. Pasini, and J. Angeles. 2010. "Optimum Design of a Compliant Uniaxial Accelerometer." *Journal of Mechanical Design* 132 (4): 041011-1–041011-8.
- Enevoldsen, I., and J. D. Sørensen. 1994. "Reliability-Based Optimization in Structural Engineering." *Structural Safety* 15 (3): 169–196.
- Engesser, M., A. Franke, M. Maute, D. Meisel, and J. Korvink. 2010. "A Robust and Flexible Optimization Technique for Efficient Shrinking of MEMS Accelerometers." *Microsystem Technologies* 16: 647–654.

- Haftka, R. T., Z. Gürdal, and M. P. Kamat. 1990. *Elements of Structural Optimization*. Dordrecht: Kluwer Academic Publishers.
- Hasofer, A. M., and N. C. Lind. 1974. "Exact and Invariant Second-Moment Code Format." *Journal of the Engineering Mechanics Division* 100 (1): 111–121.
- Kaajakari, V. 2009. *Practical MEMS*. Las Vegas, NV: Small Gear Publishing.
- Kharmanda, G., N. Olhoff, A. Mohamed, and M. Lemaire. 2004. "Reliability-Based Topology Optimization." *Structural and Multidisciplinary Optimization* 26: 295–307.
- Kovacs, G. T. 1998. *Micromachined Transducers Sourcebook*. New York: McGraw-Hill.
- Krishnan, G., C. U. Kshirsagar, G. K. Ananthasuresh, and N. Bhat. 2007. "Micromachined High-Resolution Accelerometers." *Journal of Indian Institute of Science* 87 (3): 333–361.
- Kroese, D. P., T. Taimre, Z. I. Botev. 2011. *Handbook of Monte Carlo Methods*. Hoboken, NJ: John Wiley & Sons.
- Lee, J.-O., Y.-S. Yang, and W.-S. Ruy. 2002. "A Comparative Study on Reliability-Index and Target-Performance-Based Probabilistic Structural Design Optimization." *Computers & Structures* 80 (3-4): 257–269.
- Liu, G. J., T. Jiang, and A. L. Wang. 2009. "Robust Optimization of an Accelerometer Considering Fabrication Errors." *Materials Science Forum* 628: 353–356.
- Liu, P.-L., and A. D. Kiureghian. 1991. "Optimization Algorithms for Structural Reliability." *Structural Safety* 9 (3): 161–177.
- Madou, M. J. 2002. *Fundamentals of Microfabrication: The Science of Miniaturization*. Boca Raton, FL: CRC Press.
- Madsen, H. O., and S. L. N. Krenk. 2006. *Methods of Structural Safety*. Mineola, NY: Dover Publications.
- Maute, K., and D. M. Frangopol. 2003. "Reliability-Based Design of MEMS Mechanisms by Topology Optimization." *Computers & Structures* 81 (8-11): 813–824.
- Mukherjee, T., Y. Zhou, and G. Fedder. 1999. "Automated Optimal Synthesis of Microaccelerometers." In 12th IEEE International Conference on Micro Electro Mechanical Systems (MEMS 99) 326–331.
- Nguyen, T. H., J. Song, and G. H. Paulino. 2010. "Single-Loop System Reliability-Based Design Optimization Using Matrix-Based System Reliability Method: Theory and Applications." *Journal of Mechanical Design* 132 011005: 1–11.
- Qiao, D., G. Pang, M.-K. Mui, and D. Lam. 2009. "A Single-Axis Low-Cost Accelerometer Fabricated Using Printed-Circuit-Board Techniques." *IEEE Electron Device Letters* 30 (12): 1293–1295.
- Rodrigues, J., A. Teves, A. Passaro, L. Góes, E. Silva, and C. Mateus. 2011. "Static Mechanical Analysis of a Silicon Bulk-Micromachined Accelerometer." In Proceedings of the 21st Brazilian Congress of Mechanical Engineering (COBEM).
- Roylance, L. M., and J. B. Angell. 1979. "A Batch-Fabricated Silicon Accelerometer." *IEEE Transactions on Electron Devices* 26: 1911–1917, December 1979.
- Schuëller, G., and H. Jensen. 2008. "Computational Methods in Optimization Considering Uncertainties—An Overview." *Computer Methods in Applied Mechanics and Engineering* 198 (1): 2–13.
- Seidel, H., H. Riedel, R. Kolbeck, G. Mück, W. Kupke, and M. Königer. 1990. "Capacitive Silicon Accelerometer with Highly Symmetrical Design." *Sensors and Actuators A: Physical* 21 (1-3): 312–315.
- Selvakumar, A., F. Ayazi, and K. Najafi. 1996. "A High Sensitivity z-Axis Torsional Silicon Accelerometer." In: Electron Devices Meeting, 1996. IEDM '96. International. [S.l.: s.n.], p. 765–768.
- Silva, M., D. A. Tortorelli, J. A. Norato, C. Ha, and H.-R. Bae. 2010. "Component and System Reliability-Based Topology Optimization Using a Single-Loop Method." *Structural and Multidisciplinary Optimization* 41: 87–106.
- Svanberg, K. 1987. "The Method of Moving Asymptotes—A New Method for Structural Optimization." *International Journal for Numerical Methods in Engineering* 24 (2): 359–373.
- Tu, J., K. K. Choi, and Y. H. Park. 1999. "A New Study on Reliability-Based Design Optimization." *Journal of Mechanical Design* 121 (4): 557–564.
- Yazdi, N., and K. Najafi. 2000. "An all-Silicon Single-Wafer Micro-G Accelerometer with a Combined Surface and Bulk Micromachining Process." *Journal of Microelectromechanical Systems* 9 (4): 544–550.

Appendix

The parametric optimization algorithm based on RBDO, implemented in this work, requires the calculation of the derivatives of the objective function and constraints (sensitivity analysis). Since the FORM approach has been adopted, the sensitivity of probabilistic criteria can be calculated analytically (Allen and Maute 2004), as follows.

The derivative of the probability of failure P_f with respect to the design variable s_i depends on the derivative of β with respect to the design variable s_i which, since reliability is determined from the RIA, is given by:

$$\frac{\partial \beta}{\partial s_i} = \frac{\partial \left(\sqrt{\mathbf{u}^* T \mathbf{u}^*} \right)}{\partial \mathbf{u}^*} \frac{\partial \mathbf{u}^*}{\partial s_i} = \frac{1}{\beta} \mathbf{u}^* \frac{\partial \mathbf{u}^*}{\partial s_i} \quad (\text{A1})$$

where \mathbf{u}^* denotes the MPFP, which can be found by solution of the optimization problem of Equation (2). Thus, from the Kuhn–Tucker conditions (Haftka, Gürdal, and Kamat 1990), this solution is given as:

$$\mathbf{u}^* = -\beta \frac{\frac{dQ}{d\mathbf{u}}}{\left\| \frac{dQ}{d\mathbf{u}} \right\|} \quad (\text{A2})$$

where Q is the considered limit state function.

Thus, Equation (A1) can be written as:

$$\frac{\partial \beta}{\partial s_i} = - \frac{\frac{dQ}{d\mathbf{u}}}{\left\| \frac{dQ}{d\mathbf{u}} \right\|} \frac{\partial \mathbf{u}^*}{\partial s_i} \quad (\text{A3})$$

The derivatives of $dQ/d\mathbf{u}$ and $\partial \mathbf{u}^*/\partial s_i$ can be written in terms of the original random variable \mathbf{r} , as follows:

$$\frac{dQ}{d\mathbf{u}} = \frac{dQ}{d\mathbf{r}} \frac{dT_{\mathbf{u}}^{-1}(\mathbf{u})}{d\mathbf{u}} \quad (\text{A4})$$

$$\frac{\partial \mathbf{u}^*}{\partial s_i} = \frac{dT_{\mathbf{u}}(\mathbf{r}^*)}{d\mathbf{r}} \frac{d\mathbf{r}}{ds_i} \quad (\text{A5})$$

where $T_{\mathbf{u}}$ is a transformation operator that makes the middle point in r -space corresponding to the origin in u -space.

The continuation of this derivation depends on the type of the design variable s_i , which can be deterministic or not. If a deterministic variable is considered, total variation of the limit state function Q with respect to the design variable s_i is zero (Allen *et al.* 2004).

Then, the following expression is formulated from Equation (A3):

$$\frac{d\beta}{ds_i} = \frac{1}{\left\| \frac{dQ}{d\mathbf{u}} \right\|} \frac{dQ}{ds_i} \quad (\text{A6})$$

where the term dQ/ds_i is the deterministic sensitivity of the limit state function Q .

Otherwise, for non-deterministic variables the sensitivity of the reliability index β is derived as:

$$\frac{\partial \beta}{\partial s_i} = \frac{1}{\beta} \mathbf{u}^* \frac{\partial \mathbf{u}^*}{\partial s_i} = \frac{1}{\beta} \mathbf{u}^* \frac{dT_{\mathbf{u}}(\mathbf{r}^*, \mathbf{s})}{ds_i} \quad (\text{A7})$$

The sensitivity analysis in PMA is easier to calculate than in RIA, since the performance target of the PMA is simply the value of the limit state function in MPTP. Then, the sensitivity of the performance target for PMA is the same as the sensitivity of the limit state function Q with respect to the design variable s_i , *i.e.* dQ/ds_i .